JOURNAL OF AGRICULTURAL AND FOOD CHEMISTRY

pubs.acs.org/JAFC



Article

# Spatiotemporal Dynamics of Polyphenolic Compounds in *Musa* spp. during Ripening Revealed by Mass Spectrometry Imaging

Hiroko Shinoda, Shiho Ishimoto, Eiichiro Fukusaki, and Shuichi Shimma*

Cite This: https://doi.org/10.1021/acs.jafc.5c06674

Read Online

ACCESS | Metrics & More | Article Recommendations | Supporting Information

**ABSTRACT:** Bananas (*Musa* spp.) are climacteric fruits that ripen after harvest and undergo further softening and browning, including the generation of melanin-derived black "sugar spots" on the peel via the reaction of polyphenolic compounds, such as L-DOPA, a tyrosine metabolite. Although polyphenol-related metabolite levels are altered in bananas, data visualizing localization changes while preserving spatial information have not been reported. In this study, we visualized polyphenol-related metabolites at each ripening stage using mass spectrometry imaging. We found that the L-DOPA content decreased with ripening, the dopamine content increased with banana sugar spot formation and then decreased, and tyrosine and dopaquinone contents were not related to the ripening stage. L-DOPA and dopamine were localized in the peel, whereas tyrosine and dopaquinone levels decreased in the pulp (center) and peel and increased in the outer pulp. These findings provide insights into the polyphenolic compounds underlying banana sugar spots and the melanin synthesis pathway.

**KEYWORDS:** *bananas, mass spectrometry imaging, sugar spots, polyphenol-related compounds, ripening stages*



## INTRODUCTION

Banana (*Musa* spp.) is an herbaceous plant of the family *Musaceae* that is produced in more than 130 countries worldwide with a production of over 145 million tons.[1] Bananas are highly nutritious and contain abundant nutrients, such as carbohydrates and amino acids. In addition, because of their affordable price, bananas are the most commonly purchased fruit per household in Japan, with each household purchasing approximately 20 kg of bananas per year.[2]

Bananas are a climacteric fruit that continue to ripen after harvest. Banana ripening is divided into seven stages with harvesting and transportation occurring during the first stage when the entire banana is green. To prepare them for shipment, green bananas are harvested, washed, and selected. They are then placed in low-temperature hypoxic storage to induce dormancy before being transported by sea to consumers. After transportation, bananas are awakened from dormancy and artificially treated with ethylene gas for ripening, with the green tip remaining in the fourth stage of ripening before being placed on the market. Further ripening results in softening, the appearance of black spots (called "sugar spots"), and browning. At the seventh stage, a brownish coloration of the entire crop is observed. Since consumer acceptability depends primarily on the appearance of the product, banana browning is one of the causes of reduced consumer purchases.[3,4] Because metabolite changes are involved in softening and browning, it is important to examine endogenous metabolites at each ripening stage.[5]

The pathways of melanin synthesis and its related metabolites, which are components of sugar spots, are shown in Figure 1. In this figure, sugar spots and browning in banana peels are caused by the oxidation of polyphenolic compounds such as L-DOPA, which is a metabolite of the amino acid tyrosine, followed by further polymerization reactions to produce melanin via dopaquinone.[6] Reports indicate that L-DOPA in banana peels is decarboxylated and also undergoes oxidation and polymerization via dopamine to synthesize melanin.[7]

Conventional methods for analyzing metabolites in bananas include gas chromatography−mass spectrometry (GC−MS) and liquid chromatography−mass spectrometry (LC−MS). Using these methods, changes in the metabolite content of bananas treated using different ripening methods have been analyzed.[8] Conventional methods require milling to extract metabolites from bananas, which does not provide accurate spatial information regarding metabolite distribution. In addition, the distribution of metabolites within small sugar spots that appear locally is difficult to clarify.[9,10]

Therefore, we focused on mass spectrometry imaging (MSI), a technique that can visualize the distribution of target compounds by combining 2D spatial information obtained through optical microscopy with the results of mass spectrometry at each point on a sample slice. MSI can be used to visualize the distribution of a compound of interest by combining 2D spatial information obtained via optical microscopy with the results of mass spectrometry at each point within a sample section. In particular, matrix-assisted laser desorption/ionization (MALDI) can analyze compounds over a wide mass range in a single measurement while

Received: May 26, 2025
Revised: October 6, 2025
Accepted: October 6, 2025

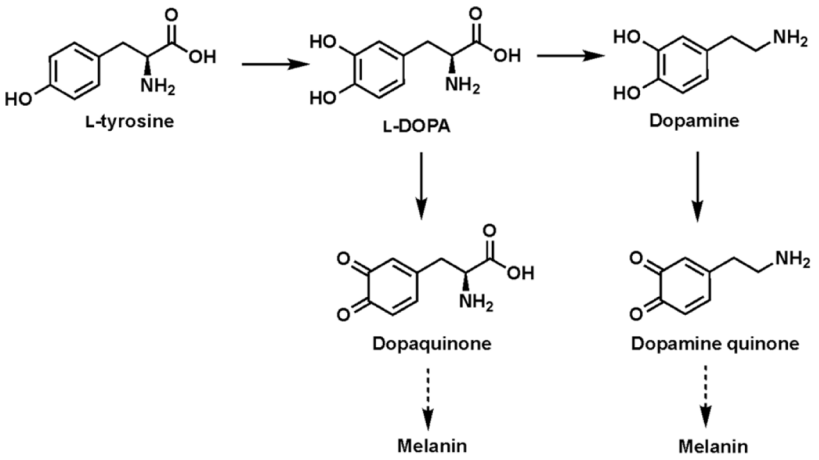


**Figure 1.** Melanin synthesis pathway using tyrosine as a substrate and its related metabolites.

maintaining spatial information and directly detecting target metabolites in a chemically specific manner.[11−13]

The objective of this study was to reveal the mechanism underlying sugar spot formation, which causes banana browning, by visualizing the localization of polyphenol-related metabolites based on the tyrosine content at each ripening stage using MSI. To achieve this, we first optimized pretreatment methods using banana samples and analyte standards. Next, we visualized the distribution of target compounds at each ripening stage using MALDI-MSI analysis under the optimized conditions. The findings presented here can help guide the development of new biomarkers for fruit ripening and quality control.

## MATERIALS AND METHODS

**Chemicals and Reagents.** Methanol, trifluoroacetic acid (TFA), formic acid, triethylamine (TEA), and 2-propanol were purchased from Fujifilm Wako Pure Chemical Co. The MALDI method utilized $\alpha$-cyano-4-hydroxycinnamic acid ($\alpha$-CHCA, 99%), 2,5-dihydroxybenzoic acid (DHB), 2,4,6-triphenylpyrylium tetrafluoroborate (TPP), and 2,4-diphenylpyranilium tetrafluoroborate (DPP) as matrices, all of which were purchased from Merck (Darmstadt, Germany). The derivatization reagent 4-(anthracen-9-yl)-2-fluoro-1-methylpyridin-1-ium iodide (FMP-10) was purchased from Tag-ON (Uppsala, Sweden). When handling toxic and hazardous chemicals, protective eyewear, gloves, and a lab coat were worn, and all reagent handling was performed within a fume hood. Ultrapure water was prepared on demand using an ultrapure water generator (Genpure UV-TOC × CAD PLUS; Thermo Fisher Scientific, Waltham, MA, USA). The banana cultivar Cavendish (*Musa* spp.) grown in the Philippines by Farmind Corporation (Tokyo, Japan) was used for the experiments.

**Ripening, Sampling, and Color Measurement Methods.** The banana samples were green prior to ethylene gas treatment, and ripening was initiated artificially. The bananas were placed in an incubator at 13 °C until the start of ripening, and ethylene treatment was performed by supplying air containing 400 ppm of ethylene at 1000 mL/min for 24 h to the banana samples in 45 L polyethylene bags at room temperature (21 °C) (Figure S1). The dilution rate was 0.022/min. The plants were then left to ripen at room temperature (20 °C). One sample was collected every 24 h for a total of 5 days after ethylene treatment. The untreated sample was designated as the Day 0 sample, and the ethylene-treated samples were designated Days 1−5, for a total of six samples. Each banana sample was analyzed at three points using a spectrophotometer (CM-2600d; Konica Minolta, Tokyo, Japan) in the $L^*a^*b^*$ color space. The center of the banana was cut to a thickness of 1 cm and a width of 1 cm to form a fan shape with a central angle of 60°. The sample was immediately placed in a 15 mL Falcon tube and frozen in liquid nitrogen. Frozen samples were placed in 50 mL Falcon tubes and stored in a light-shielded freezer at −80 °C until sectioning. Banana peel samples from Day 10, which had more sugar spots, were placed in 15 mL Falcon tubes, frozen in liquid nitrogen, and stored at −80 °C. Banana peel samples from Day 11, which had even more sugar spots (visual examination), were frozen in 15 mL Falcon tubes and stored at −80 °C.

**Banana Section Preparation.** The bananas were ripened as described in the previous section and frozen in liquid nitrogen. Sections (40-$\mu$m-thick) were prepared from the frozen samples using a cryomicrotome (CM1950; Leica Biosystems, Nussloch, Germany) at −30 °C. The frozen sections were then transferred to a cryofilm (SECTION-LAB, Yokohama, Japan). After being thawed to room temperature, the cryofilm with the samples was fixed on indium tin oxide (ITO)-coated glass (Matsunami Glass, Osaka, Japan) using conductive nonwoven fabric double-sided tape (3M, St. Paul, US). The samples were allowed to dry in 50 mL centrifuge tubes containing silica gel.

**Optimization of the Derivatization Method.** The derivatization method for the target metabolites—tyrosine, L-DOPA, dopamine, and dopaquinone—was optimized using the derivatization reagents FMP-10, TPP, and DPP.[14,15] Derivatization reactions were performed using each reagent to investigate the detection intensity and determine whether the overlap was caused by peaks with $m/z$ values close to the detection peak of the target metabolite. FMP-10 solution (1.8 mg/mL) was prepared by using 70% methanol as the solvent. Then, 500 $\mu$L of FMP-10 solution per banana section was sprayed evenly over the entire section using an airbrush (Procon BOY SQ; GSI Creos, Tokyo, Japan).

The TPP solution was prepared as a solvent by mixing methanol, ultrapure water, and triethylamine at a volume ratio of 1,200:300:1 to obtain a concentration of 1.3 mg/mL. Then, 500 $\mu$L of TPP solution per banana section was sprayed evenly over the entire section using an airbrush (P-270, Procon BOY SQ). Derivatization was then performed by placing the sections at room temperature for 40 min under light-shielded conditions. The reaction time was overnight.

A DPP stock solution was prepared using methanol as the solvent at 10 mg/mL. The DPP solution was prepared by adding 32 $\mu$L of DPP stock solution to 368 $\mu$L of diluted solvent at a volume ratio of water:methanol:TEA = 600:900:1. A total of 200 $\mu$L of DPP solution per banana section was sprayed evenly over the entire section by using an airbrush. The reaction time was overnight.

**Matrix Application.** When FMP-10 was used as the derivatization reagent, $\alpha$-CHCA was used as the matrix. In the vacuum sublimation method, $\alpha$-CHCA heated to 250 °C was evaporated at a thickness of 0.7 $\mu$m onto ITO glass containing the frozen sections, which were placed by using a vacuum sublimation system (iMLayer; Shimadzu Corporation, Kyoto, Japan). In the spray method, a mixture of acetonitrile, ultrapure water, 2-propanol, and 0.1% formic acid at a volume ratio of 30:60:10:1 was used as the solvent. Then, 500 $\mu$L of


https://doi.org/10.1021/acs.jafc.5c06674
J. Agric. Food Chem. XXXX, XXX, XXX−XXX

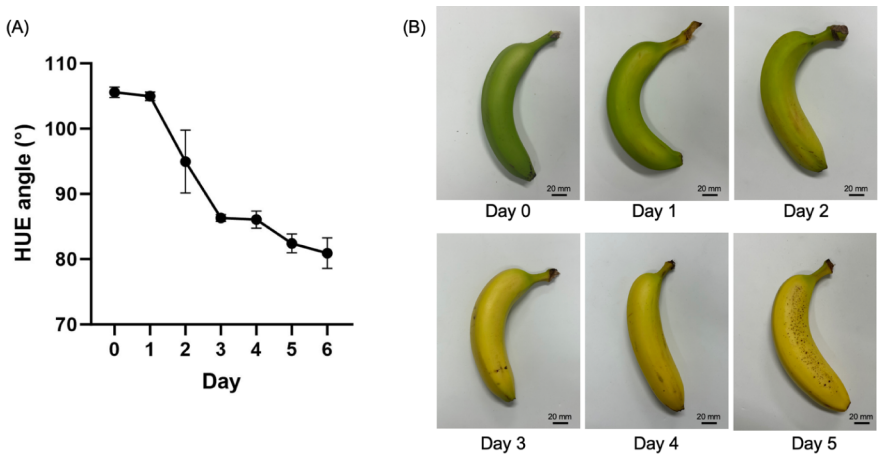


**Figure 2.** Changes in banana peel at different stages of ripening. (A) Change in HUE angle ($n$ = 4) and (B) banana color change at each ripening stage. A yellowish hue is observed from Day 2 to Day 3, and sugar spots appear on Day 5. Error bars: SD, biological replicate: $n$ = 3, scale bars: 20 mm.

$\alpha$-CHCA solution prepared at 5 mg/505 $\mu$L per section was applied uniformly to the entire section by using an airbrush.

When DPP and TPP were used as the derivatization reagent, DHB was used as the matrix. Briefly, a 19 mg/505 $\mu$L DHB solution was prepared by mixing methanol, ultrapure water, and 1% formic acid at a volume ratio of 80:20:1. Then, 200 $\mu$L of DHB solution per section was evenly sprayed onto the entire section using an airbrush.

**MALDI-MSI Analysis.** MALDI-MSI analysis was performed using an iMScope QT (Shimadzu Corporation) with a laser diameter of 25 $\mu$m. All mass spectra were acquired in positive ion mode. The $m/z$ range was 400−740 when FMP-10 and TPP were used as derivatizing reagents and 300−600 when DPP was used. The iMScope QT is a quadrupole time-of-flight mass spectrometer equipped with an optical microscope and an atmospheric pressure MALDI ion source using a Nd:YAG (neodymium: yttrium aluminum garnet) laser ($\lambda$ = 355 nm, 1 kHz). When we performed the analysis, the laser energy was 62 (dimensionless parameter), and the number of laser shots per pixel was 50.

**Data Analysis of MS Images.** The software IMAGEREVEAL MS (version 1.20.0.10960; Shimadzu Corp.) was used for data analysis. Images of each polyphenol-related metabolite were obtained for each $m/z$ peak.

## RESULTS AND DISCUSSION

**Ripening Stages and Color Measurement of Bananas.** Figure 2 shows photographs of bananas ripened by using the method described previously, and their colors were measured according to the $L^*a^*b^*$ color space. The HUE angle is a derived value that uniformly represents chromaticity based on the values obtained from $a^*b^*$ and is calculated by using eqs 1−3. HUE angles of approximately 90° correspond to yellow, and those of approximately 180° correspond to green.[16]

$$\text{THETA} = \left( \frac{\text{ATAN}\left(\frac{b^*}{a^*}\right)}{6.2832} \right) \times 360 \quad (1)$$

$$\text{HUE} = \text{THETA} \ (\text{if } a^* > 0) \quad (2)$$

$$\text{HUE} = \text{THETA} + 180 \ (\text{if } a^* < 0) \quad (3)$$

As ripening progressed, the HUE angle decreased, falling below 90° for the first time on Day 3 (Figure 2A). This tendency was consistent with the result in ref 12. The color change was particularly pronounced from Days 1 to 3 after ethylene treatment. Sugar spots appeared on Day 5 (Figure 2B). On Day 5, the number of sugar spots was more than 100. On the other hand, we could not confirm sugar spots before Day 5.

**Optimization of Derivatization Reagents.** When using MSI for the surface analysis of sections, the detection sensitivity may be low if the desorption/ionization efficiency of the target metabolite is low without derivatization (Figure S2).[17] TPP and DPP are pyrylium salts that react with primary amines to form $N$-alkylpyridinium or $N$-arylpyridinium derivatives. Tyrosine, L-DOPA, dopamine, and dopaquinone are all primary amines, and the use of pyrylium salts as derivatizing reagents is expected to improve their detection sensitivity. In addition, FMP-10 has a reactive matrix of fluoromethylpyridinium, which reacts with primary and secondary amines via aromatic nucleophilic substitution, thus improving the detection sensitivity of the target metabolite.[18] Therefore, we investigated whether the application of derivatizing reagents FMP-10, TPP, and DPP to banana sections increased the detection intensity. Table 1 lists the $m/z$ values of the polyphenol-related compounds when each derivatization reagent was used, and Figure 3 shows the reaction equations for each derivatization reagent.

**Table 1. $m/z$ Values of Polyphenol-Related Metabolites Using Each Derivatization Reagent**

| | FMP-10 | TPP | DPP |
|---|---|---|---|
| Tyrosine | 449.18 | 472.18 | 396.16 |
| L-DOPA | 465.18 | 488.18 | 412.15 |
| Dopamine | 421.19 | 444.19 | 368.16 |
| Dopaquinone | 463.17 | 486.17 | 410.14 |


https://doi.org/10.1021/acs.jafc.5c06674
J. Agric. Food Chem. XXXX, XXX, XXX−XXX

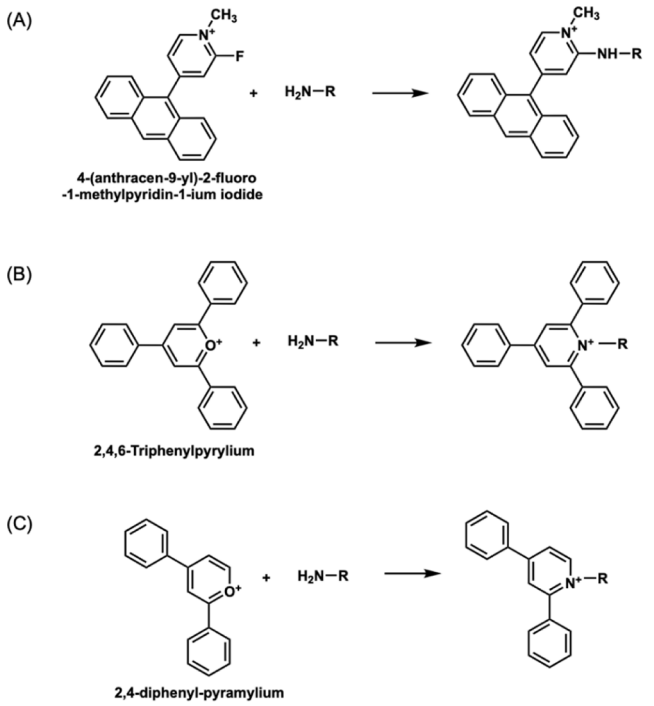


**Figure 3.** Reaction scheme of each derivatization reagent.

The detection intensities of tyrosine, L-DOPA, dopamine, and dopaquinone at the corresponding $m/z$ values after derivatization were compared, and the results are shown in Figure S3. After derivatization with FMP-10 (Figure S3A), overlapping peaks were observed for L-DOPA and dopamine. After derivatization with TPP (Figure S3B), the detection intensity was low, and the peaks were not separated, which may indicate that the correct intensity was not detected. Although a peak for dopaquinone could be detected, its intensity was low (Figure S3C). To confirm the ionization efficiency using DPP, we obtained mass spectra using standard samples and compared the intensities. In this experiment, we can detect the peaks of derivatized tyrosine, dopamine, and L-DOPA. The peak intensity of dopamine was the highest among these samples (Figure S4).

**Visualization of Polyphenol-Related Metabolite Localization in Bananas at Each Ripening Stage.** Derivatization was performed using DPP as described in previous sections, and MSI analysis was performed to visualize the localization of polyphenol-related metabolites in bananas at each ripening stage. The results are shown in Figure 4. To confirm whether derivatized compounds were detected in the banana samples, we obtained the product ion spectrum (Figure S5). We could detect the product ion peaks for tyrosine, L-DOPA, dopamine, and dopamine quionone. For dopaquinone, we could not detect the product ion peak due to its low concentration.

MSI analysis revealed that the distribution of tyrosine decreased in the peel and pulp center and increased in the outer pulp as ripening progressed (Figure 4A and regions of interest are shown in Figure S6). L-DOPA localization decreased in intensity across all banana sections as ripening progressed following ethylene treatment, while a high-intensity distribution was observed in the peel at all ripening stages (Figure 4B). Dopamine was initially localized to the peel (Days 0 and 1) but later appeared in the pulp on Days 3 and 5

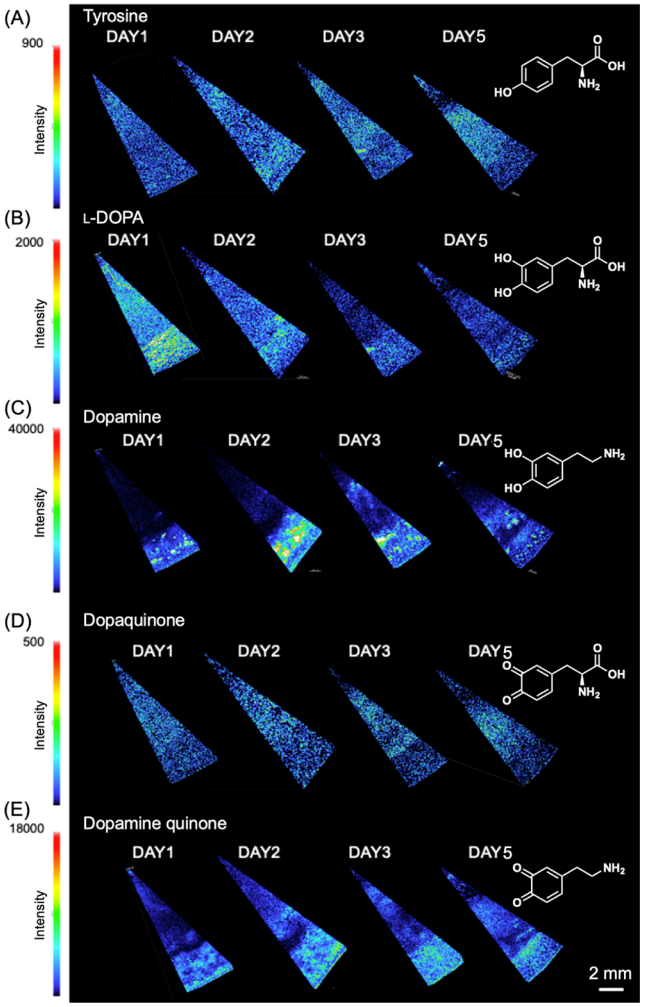


**Figure 4.** Localization of polyphenol-related metabolites in bananas at different ripening stages: (A) Tyrosine, (B) L-DOPA, (C) dopamine, (D) dopaquinone, and (E) dopamine quinone.

(Figure 4C). Dopaquinone showed reduced intensity in the peel and pulp center and increased intensity outside the pulp as ripening progressed (Figure 4D). Dopamine quinone was predominantly distributed in the peel and appeared only slightly in the pulp (Figure 4E).

The detection intensity of L-DOPA decreased with ripening. In contrast, the dopamine intensity increased with ripening and decreased when sugar spots appeared (Day 5). The intensity of dopamine quinone increased with ripening, particularly in the pith. The detection intensities of tyrosine and dopaquinone were not correlated with ripening (Figure S7).

A study has indicated that melanin, which causes sugar spots, is synthesized by L-DOPA, which is synthesized from tyrosine via dopaquinone.[19] Since dopamine and dopamine quinone, which are intermediate products of the melanin synthesis pathway via dopamine, are abundantly distributed on the peel surface where sugar spots appear, it is thought that L-DOPA produces dopamine, which triggers the production of melanin that causes sugar spots. Bananas changed from green to yellow on Day 3; however, this change was not correlated with polyphenol-related metabolites.

**Visualization of the Localization of Polyphenol-Related Metabolites in Banana Sugar Spots.** Derivatization was performed using DPP as described in a previous


https://doi.org/10.1021/acs.jafc.5c06674
J. Agric. Food Chem. XXXX, XXX, XXX−XXX

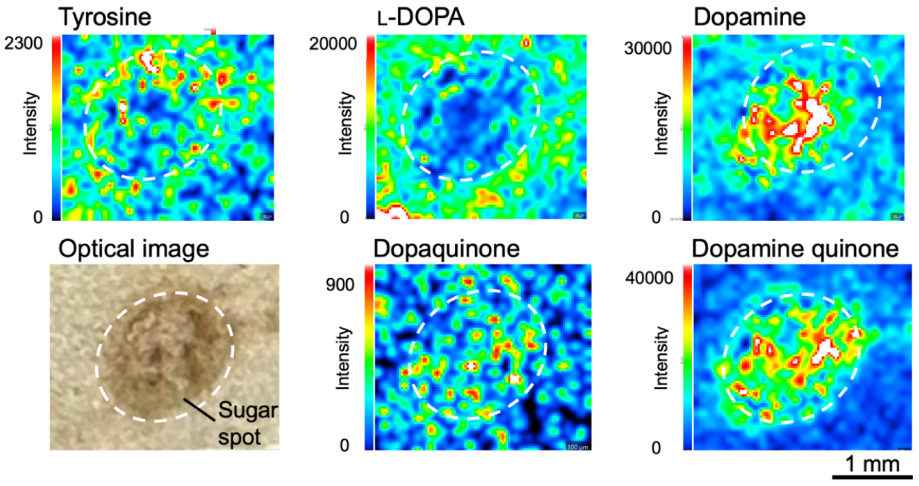


**Figure 5.** Localization of polyphenol-related metabolites in sugar spots.

section, and MSI analysis was performed to visualize the localization of polyphenol-related metabolites with a focus on sugar spots. The results are shown in Figure 5.

Localization analysis of metabolites in the melanin synthesis pathway in banana sugar spots yielded interesting results. Visualization using MSI revealed that tyrosine and L-DOPA, precursors in the melanin synthesis pathway, were localized in the outer region of the sugar spots, whereas their downstream metabolites, dopaquinone, dopamine, and dopamine quinone, were localized inside the sugar spots.[7] In particular, strong localization within sugar spots was observed for dopamine and dopamine quinone.

This spatial distribution pattern of metabolites suggests a sophisticated mechanism underlying metabolic regulation of the melanin synthesis pathway. The presence of spatially separated precursors and subsequent metabolites in the synthesis pathway indicates that this pathway is regulated in a tissue-specific manner.[20] Such spatial control may function as a regulatory mechanism that allows for efficient melanin synthesis while preventing the production of more melanin than necessary.

L-DOPA was not observed within the sugar spots; however, it was observed outside the sugar spots, and its presence or absence was clear. This suggests that L-DOPA was stable outside the sugar spot on the yellow peel owing to the low pH; however, as the pH of the banana increased with ripening, L-DOPA became unstable, and the decarboxylation reaction proceeded at a faster rate, thereby producing dopamine, which led to this extreme distribution.[4,21]

The significant accumulation of dopamine and dopamine quinone within the sugar spots also suggests that a group of enzymes that catalyze the synthesis of these substances, specifically in this region, is highly active.[22] This finding also suggested an important clue regarding the regulatory mechanisms of melanin synthesis during banana ripening.

Furthermore, spatial control of this pathway may have evolved as a physiological defense mechanism during fruit ripening. The precise regulation of sugar spot formation suggests that this phenomenon plays an important role in fruit physiology.[23]

These findings have the potential to lead to the development of new biomarkers for fruit ripening and quality control, which could contribute to the improvement of postharvest quality control techniques for agricultural crops. Further elucidation of the molecular mechanisms involved in the spatial regulation of this pathway is required.

To summarize, in this study, we visualized the localization of endogenous polyphenol-related metabolites in bananas at each ripening stage for the first time using MSI. The results showed that L-DOPA and dopamine were distributed throughout the peel. In contrast, tyrosine and dopaquinone did not show extreme localization. The detection intensity of L-DOPA decreased with ripening, whereas that of dopamine increased and then decreased with the appearance of sugar spots. Moreover, the progression of aging was not correlated with the detection intensities of tyrosine and dopaquinone.

We hypothesized that melanin formation occurs through two pathways: one from L-DOPA via dopaquinone and the other via dopamine. Based on the results obtained in this study, the pathway to generate L-DOPA from tyrosine via the tyrosinase reaction may be consistent with that used to generate dopamine. Although the dopaquinone pathway has been identified as a pathway for synthesizing melanin in plants,[24] the present results were unexpected. In the future, the melanin formation pathway in bananas will be elucidated by focusing on the peel surface prior to sugar spot formation.

## ■ ASSOCIATED CONTENT

### Data Availability Statement

The data that support the findings of this study are available on request from the corresponding author, S.S.

### Supporting Information

The Supporting Information is available free of charge at https://pubs.acs.org/doi/10.1021/acs.jafc.5c06674.

Ethylene gas treatment of banana; mass spectra of with and without derivatization; MS/MS analysis of target compounds; relationship between ripening progression and ion intensities of each metabolite (PDF)

## ■ AUTHOR INFORMATION

### Corresponding Author

**Shuichi Shimma** − *Department of Biotechnology, Graduate School of Engineering, The University of Osaka, Suita, Osaka 5650871, Japan; The University of Osaka and Shimadzu Omics Innovation Research Laboratory and Institute for Open and Transdisciplinary Research Initiatives, The University of Osaka, Suita, Osaka 5650871, Japan;*



https://doi.org/10.1021/acs.jafc.5c06674
J. Agric. Food Chem. XXXX, XXX, XXX−XXX

orcid.org/0000-0002-4699-6590; Email: sshimma@bio.eng.osaka-u.ac.jp; Fax: +81-6-6879-7418

### Authors

**Hiroko Shinoda** − *Department of Biotechnology, Graduate School of Engineering, The University of Osaka, Suita, Osaka 5650871, Japan*

**Shiho Ishimoto** − *Department of Biotechnology, Graduate School of Engineering, The University of Osaka, Suita, Osaka 5650871, Japan;* Present Address: Shimadzu Corporation, Nishinokyo Kuwabaracho, 1, Nakagyo-ku, Kyoto 604-8442, Japan

**Eiichiro Fukusaki** − *Department of Biotechnology, Graduate School of Engineering, The University of Osaka, Suita, Osaka 5650871, Japan; The University of Osaka and Shimadzu Omics Innovation Research Laboratory and Institute for Open and Transdisciplinary Research Initiatives, The University of Osaka, Suita, Osaka 5650871, Japan*

Complete contact information is available at: https://pubs.acs.org/10.1021/acs.jafc.5c06674

### Author Contributions

H.S. performed the measurements; E.F. and S.S. were involved in planning and supervised the work; H.S., S.I., and S.S. processed the experimental data, performed the analysis, drafted the manuscript, and designed the figures. All authors discussed the results, commented on the manuscript, and have read and agreed to the published version of the manuscript.

### Notes

The authors declare no competing financial interest.

## ■ ACKNOWLEDGMENTS

The authors thank Farmind Corporation and SC Foods Co., Ltd. for providing the banana samples. This study was financially supported by a Management Expense Grant (Nn24100000) from Osaka University.

## ■ ABBREVIATIONS

| | |
|---|---|
| DHB | 2,5-dihydroxybenzoic acid |
| DPP | 2,4-diphenylpyranilium tetrafluoroborate |
| FMP-10 | 4-(anthracen-9-yl)-2-fluoro-1-methylpyridin-1-ium iodide |
| ITO | indium tin oxide |
| MALDI | matrix-assisted laser desorption/ionization |
| MSI | mass spectrometry imaging |
| TEA | trimethylamine |
| TFA | trifluoroacetic acid |
| TPP | 2,4,6-triphenylpyrylium tetrafluoroborate |

## ■ REFERENCES

(1) Qamar, S.; Shaikh, A. Therapeutic potentials and compositional changes of valuable compounds from banana- A review. *Trends Food Sci. Technol.* **2018**, *79*, 1−9.

(2) Tsubuku, M. B. P.; *Annals Of Cheap: Bananas*. https://www.japantimes.co.jp/news/2012/11/08/business/annals-of-cheap-bananas/. accessed 26-May 2012.

(3) Pathak, S. S.; Sonawane, A.; Srinivas, A.; Pradhan, R. C. Application of Image Analysis for Detecting the Browning of Unripe Banana Slices. *ACS Food Sci. Technol.* **2021**, *1* (9), 1507−1513.

(4) Wantat, A.; Rojsitthisak, P.; Seraypheap, K. Inhibitory effects of high molecular weight chitosan coating on 'Hom Thong' banana fruit softening. *Food Packag. Shelf Life* **2021**, *29*, 100731.

(5) Yuan, Y.; Zhao, Y.; Yang, J.; Jiang, Y.; Lu, F.; Jia, Y.; Yang, B. Metabolomic analyses of banana during postharvest senescence by (1)H-high resolution-NMR. *Food Chem.* **2017**, *218*, 406−412.

(6) Romphophak, T.; Siriphanich, J.; Ueda, Y.; Abe, K.; Chachin, K. Changes in concentrations of phenolic compounds and polyphenol oxidase activity in banana peel during storage. *Food Preserv. Sci.* **2005**, *31* (3), 111−115.

(7) Palmer, J. K.; Polyphenoloxidase, B. Preparation and Properties. *Plant Physiol.* **1963**, *38* (5), 508−513.

(8) Tallapally, M.; Sadiq, A. S.; Mehtab, V.; Chilakala, S.; Vemula, M.; Chenna, S.; Upadhyayula, V. GC-MS based targeted metabolomics approach for studying the variations of phenolic metabolites in artificially ripened banana fruits. *LWT* **2020**, *130*, 109622.

(9) Choehom, R.; Ketsa, S.; van Doorn, W. G. Senescent spotting of banana peel is inhibited by modified atmosphere packaging. *Postharvest Biol. Biotechnol.* **2004**, *31* (2), 167−175.

(10) Trakulnaleumsai, C.; Ketsa, S.; van Doorn, W. G. Temperature effects on peel spotting in 'Sucrier' banana fruit. *Postharvest Biol. Biotechnol.* **2006**, *39* (3), 285−290.

(11) Caprioli, R. M.; Farmer, T. B.; Gile, J. Molecular imaging of biological samples: Localization of peptides and proteins using MALDI-TOF MS. *Anal. Chem.* **1997**, *69* (23), 4751−4760.

(12) Ishimoto, S.; Fukusaki, E.; Shimma, S. Mass spectrometry imaging of gamma-aminobutyric acid and glutamic acid decarboxylase reactions at various stages of banana ripening. *J. Biosci. Bioeng.* **2025**, *139* (1), 79−84.

(13) Shimma, S.; Sagawa, T. Microscopy and Mass Spectrometry Imaging Reveals the Distributions of Curcumin Species in Dried Turmeric Root. *J. Agric. Food Chem.* **2019**, *67* (34), 9652−9657.

(14) Shariatgorji, M.; Nilsson, A.; Fridjonsdottir, E.; Vallianatou, T.; Källback, P.; Katan, L.; Sävmarker, J.; Mantas, I.; Zhang, X.; Bezard, E.; Svenningsson, P.; Odell, L. R.; Andrén, P. E. Comprehensive mapping of neurotransmitter networks by MALDI−MS imaging. *Nat. Methods* **2019**, *16* (10), 1021−1028.

(15) Shariatgorji, M.; Nilsson, A.; Källback, P.; Karlsson, O.; Zhang, X.; Svenningsson, P.; Andren, P. E. Pyrylium Salts as Reactive Matrices for MALDI-MS Imaging of Biologically Active Primary Amines. *J. Am. Soc. Mass Spectrom.* **2015**, *26* (6), 934−939.

(16) Mclellan, M. R.; Lind, L. R.; Kime, R. W. HUE ANGLE DETERMINATIONS AND STATISTICAL ANALYSIS FOR MULTIQUADRANT HUNTER L,a,b DATA. *J. Food Qual.* **1995**, *18* (3), 235−240.

(17) Porta, T.; Lesur, A.; Varesio, E.; Hopfgartner, G. Quantification in MALDI-MS imaging: What can we learn from MALDI-selected reaction monitoring and what can we expect for imaging? *Anal. Bioanal. Chem.* **2015**, *407* (8), 2177−2187.

(18) Merdas, M.; Lagarrigue, M.; Vanbellingen, Q.; Umbdenstock, T.; Da Violante, G.; Pineau, C. On-tissue chemical derivatization reagents for matrix-assisted laser desorption/ionization mass spectrometry imaging. *J. Mass Spectrom.* **2021**, *56* (10), No. e4731.

(19) Ademakinwa, A. N.; Agunbiade, M. O. Banana peel wastes as a source of tyrosinase useful in the production of l-DOPA. *Sustainable Chem. Pharm.* **2022**, *30*, 100853.

(20) Galeazzi, M. A. M.; Sgarbieri, V. C. Substrate Specificity and Inhibition of Polyphenoloxidase (PPO) From a Dwarf Variety of Banana (Muss Cavendishii, L.). *J. Food Sci.* **1981**, *46* (5), 1404−1406.

(21) Chiwate, S. M.; Jadhav, B. T.; Nikam, S. V. Analysis of Physicochemical Changes During the Ripening of Cavendish Banana and Velchi Banana. *Curr. Agri Res.* **2023**, *11* (1), 236−243.

(22) Martinez, M. V.; Whitaker, J. R. The biochemistry and control of enzymatic browning. *Trends Food Sci. Technol.* **1995**, *6* (6), 195−200.

(23) Sui, X.; Meng, Z.; Dong, T.; Fan, X.; Wang, Q. Enzymatic browning and polyphenol oxidase control strategies. *Curr. Opin. Biotechnol.* **2023**, *81*, 102921.

(24) Cabanes, J.; García-Cánovas, F.; Lozano, J. A.; García-Carmona, F. A kinetic study of the melanization pathway between L-tyrosine and dopachrome. *Biochim. Biophys. Acta, Protein Struct. Mol. Enzymol.* **1987**, *923* (2), 187−195.